POINT SPREAD FUNCTION ESTIMATION OF HIGH RESOLUTION SPACE BORNE IMAGING SENSORS USING STELLAR SOURCE

Santhi Sree. B, Sri Sudha.S, Raghavender.N, Chandrasekaran.D, Gopala Krishna.B
Data and Product Quality Evaluation Division, Satellite Data Product Quality Assurance Group, Data Processing, Products Archival and Web Applications Area, National Remote Sensing Centre, Balanagar, Hyderabad-500037
(Email: santhisree_b@nrsc.gov.in)

KEYWORDS: Cartosat-2E; Optical butting; Stellar sources; Point spread function (PSF); Modulation transfer function (MTF).

ABSTRACT: PSF is one of the key characteristic of an optical system on which the performance of optical system depends. More accurate assessment of on-orbit PSF and derived MTF are useful in enhancing the image quality. Cartosat-2S platforms carrying high resolution imaging sensors in the optical bands namely multispectral (MX) camera with 1.6m and panchromatic (PAN) camera with 0.6m spatial resolution. During the early orbit phase stars were acquired at various locations of the array to arrive PSF characterization of the system. PSF estimated by taking16x16 pixels energy around the star position into consideration after compensating the dark current. Integrated PSF was derived using multi star occurrence at different locations of the detector array. PSF and MTF was also estimated in the earth observation mode using edge response from the image by ground based artificial targets at a contrast difference of 50% reflectance in the visible near infrared (VNIR) wavelength regions to estimate the system response. The PSF found to be within 2 to 2.5 pixels by all these observations. Image quality was observed for the images obtained at different terrains over a period with the PSF correction and found to be improved.

1. INTRODUCTION

PSF estimation is very important activity in the early orbit phase operations of high resolution imaging cameras. It enables to understand the camera or imaging device performance after the launch and accordingly fine tune the correction modules in the processing chains. Estimates made during the early phases or immediately after launch, act as reference for subsequent observations.

Cartosat-2E (C2E) is an earth observation (EO) satellite developed by the Indian Space Research Organisation (ISRO), and is the seventh in the Cartosat series. It is designed to collect high-resolution, large-scale imagery for use in urban planning, infrastructure development, utilities planning, and traffic management. The satellite was launched on 23 June 2017, along with NIUSAT and 29 other satellites, aboard a PSLV-XL rocket from Satish Dhawan Space Centre (SDSC). It is configured to provide PAN imagery with 0.6 m resolution and MX with 1.6m resolution from 500km orbit. Both sensors image an identical swath of ~10km with few seconds time delay. PAN camera operates in the wavelength region: 450-900nm and MX in four bands (Band1:450-520, Band2:520-590, Band3:620-680, Band4:770-860) covering visible and near infrared (VNIR) region. To provide improved SNR high resolution images, PAN, MX cameras were built on TDI technology/devices. The main purpose of the Cartosat-2 satellite series is the generation of imagery for cartography, environmental monitoring, disaster relief and event monitoring.

PAN sensor covers full swath of 10km with two 80stage devices. Two devices are optically butted together using mirrors to provide contiguous swath. Hence, PAN sensor has one butting region centered at 8192 pixel position, with common area of ~270 pixels. Each device has 8192 pixels/elements in a scan line. Size of each pixel is 7 µm X 7 µm. There are a total of 32 ports in PAN sensor for readout. MX sensor covers full swath of 10km with five 45 stage devices in each band. MX sensor has four butting zones with common area of ~70 pixels per butting zone. Each device has 1340 pixels/elements in a scan line. Size of each pixel is 17.6 µm X 17.6 µm. There are a total of 10 ports in MX sensor for readout.

2. STELLAR IMAGING

Various approaches are being followed by different agencies to estimate the PSF fall basically into two categories: (a) using objects or targets on the surface of the earth (like tarps, painted targets, bridges, roof tops etc) and (b) extraterrestrial objects (point objects like stars).[1],[2],[3] Estimates based on the objects on the surface of the earth get influenced by the intervening atmosphere and on the other hand it is absent while imaging extraterrestrial objects. However, extraterrestrial objects observation is a complex process, which demands accurate and stable satellite systems.

3. DATASETS

In order to characterize the spatially varying blur, stars were imaged at different locations of the full detector array. A total of four stellar imaging observations were done soon after the C2E launch, i.e. in the month of July 2017. Details of the imaging parameters are provided in Table 1. As discussed in section 1, both cameras have butting zones, PAN-1 and MX-4. Image features in butting zone may have blur with respect to the other areas.

Table 1 Details of stellar imaging

Date of Imaging	Orbit	Sensor	Star-ID	V-Mag	TDI Stages	Integration Time (msec)	Imaging Sessions	Remarks
07-Jul-17	218	PAN	6321	6.26	24	0.534	6	Non butting zone
08-Jul-17	233	PAN	6321	6.26	24	0.534	6	Butting Zone
11-Jul-17	279	MX	7840	7.11	15	0.896	6	Non butting zone
13-Jul-17	309	MX	7840	7.11	15	0.896	6	Butting Zone

3. PSF ESTIMATION METHODOLODY

The derivation of full width half maxima (FWHM) based on single star acquisition is computed. This FWHM is related to the characteristics of that specific zone based on the star position located at the detector array. The detailed procedure followed for the extraction of effective star position and normalisation of dark current and the outputs of each stage and arriving at FWHM is described below in Figure 1.

The star is identified based on the intended location by searching for maximum DN count. 11 x 11 star matrix is extracted after compensation of dark current. The spatial profile of the star is interpolated using bicubic convolution method and generated $1/10^{th}$ of two dimensional spatial pixel profile. This enables to identify the exact star energy location. The matrix is normalized to one for the identified maximum star DN . Using "shape preserving curve fitting" method ,along track and across track pixel profiles are generated. subsequently FWHM is computed for both the directions [4],[5] .

For generating detector array level integrated PSF, the qualified stars are selected based on the good DN count and symmetrical spatial profiles are considered. By integrating the selected star profiles in the spatial domain a common array level intensity profile in sub pixel level ($1/10^{th}$) is arrived. PSF in both the directions is computed using above mentioned method.

4. RESULTS & DISCUSSIONS

Total 12 star locations of PAN detector array including butting zone is providing a great opportunity of establishing integrated PSF using individual FWHM. The star 6321acquired by PAN sensor at intended positions 2000, 4000, 6000, 10000, 12000 and 14000 are observed for the intensity. The intensities vary from 384 DN counts to 750 DN counts. Any star occurrence in the data with 2 to 3 times more than dark current will provide an opportunity of deriving FWHM. Similarly, in this there are more number of stars observed in the image data as the camera is viewing the deep space. But here, to pick up the intended Star is important as the integration time for acquisition will provide the right FWHM. The star positions in the deep space data are located with the help of intended timing information in the each session to avoid any ambiguity. Table 2, details stellar observation (DN counts), and derived FWHM for different segments of array as described by the above methodology. FWHM found to be varying between 1.4 pixels to 2.3 pixels at different locations by considering both the directions which have been acquired over six sessions.

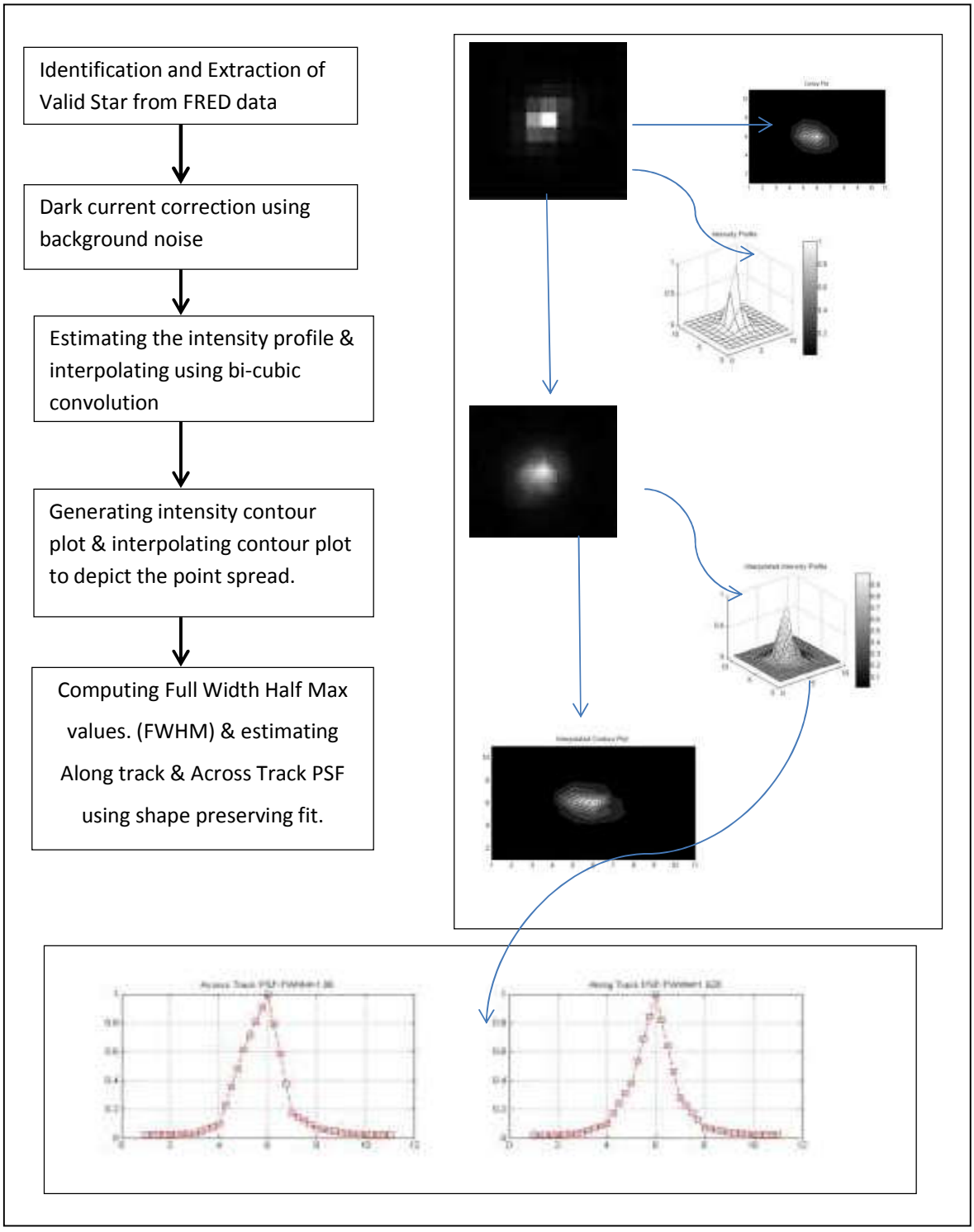

Figure 1 FWHM estimation methodology.

Table 2 Estimated FWHM for PAN sensor in non-butting zone

Ses.No	Intended star location	DN Counts	Along track FWHM	Across track FWHM
0	2000	750	1.6	1.4
1	4000	489	2.1	2.1
2	6000	384	2.3	2.4
3	10000	414	2.2	2.1
4	12000	626	1.7	1.7
5	14000	587	1.6	1.9

Table 3 Estimated FWHM for PAN sensor in butting zone

Session No	Intended star location	DN Counts	Along track FWHM	Across track FWHM
0	8014	259	1.8	2.2
1	8092	370	2.4	2.1
2	7936	553	1.8	2.1
3	8192	499	1.9	1.7
4	8292	312	2.3	1.9
5	8342	333	1.9	1.6

Similarly, Table 3 provides the details of computed FWHM near and around butting zone, which is a mid segment of the area between D1 and D2. The star locations are observed at 7936, 8014, 8092, 8192, 8292 and 8342. This stellar observation over and near butting zones is very important to understand and characterise the common area between D1 and D2. If we observe Table3. It is very clear that there is no significant deviation or degradation in the butting zone areas compared to normal detector array.

Fig2 and Fig 3 depicts the different star energy spread in the pixel level at all six different locations across detector array. The spread observed to be uniform and there were no skewed patterns. FWHM values of intensity profiles at different locations in along track and across tract direction are shown in plot1. From Plot1 it is evident that on the average of these observations the FWHM is about 2 pixels and its varying between 2.4 pixels to 1.6 pixels randomly. There is no significant linear trends observed. However at the 2000 detector position the best FWHM value is observed about 1.5 pixels and the DN counts are also observed to be relatively high compared to other sessions. All the 12 observations are used for deriving effective instrumental PSF of PAN and it is observed to be around 1.9 pixels in across track and 1.8 pixels in along track direction. This integrated PSF is compensated in the data processing chain as a base PSF for restoration process.

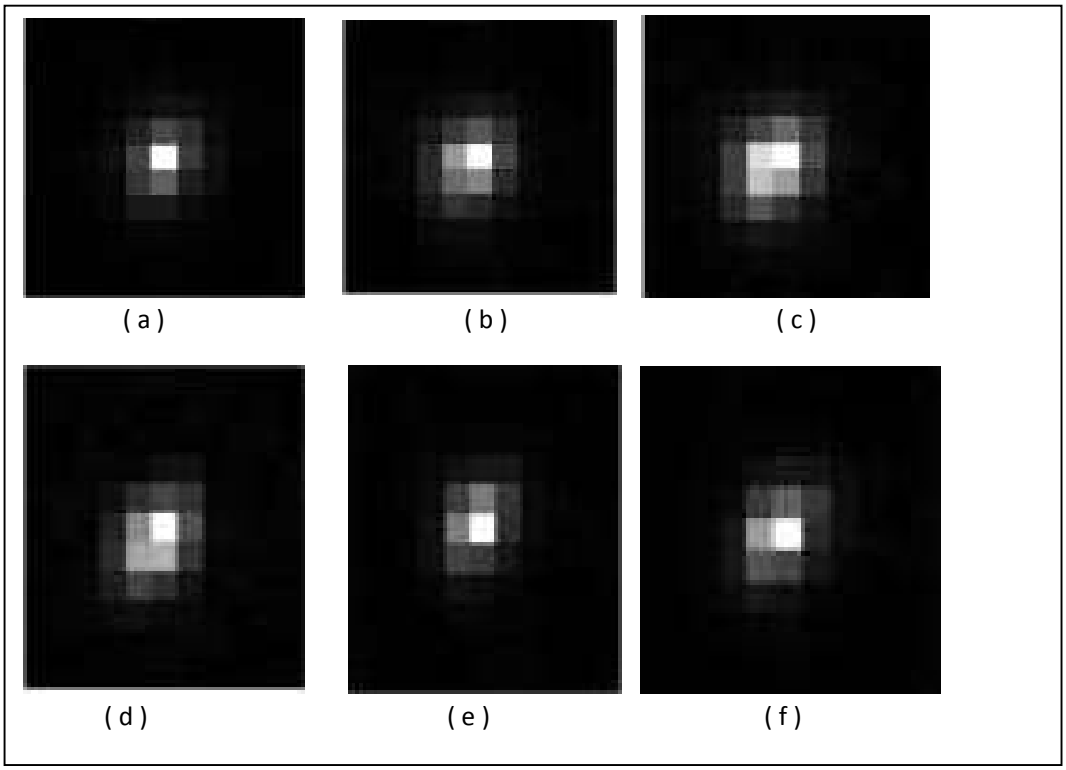

Figure 2 Star - Point Source observed by C2E PAN Sessions: 0, 1, 2, 3, 4, 5 (non butting zone)

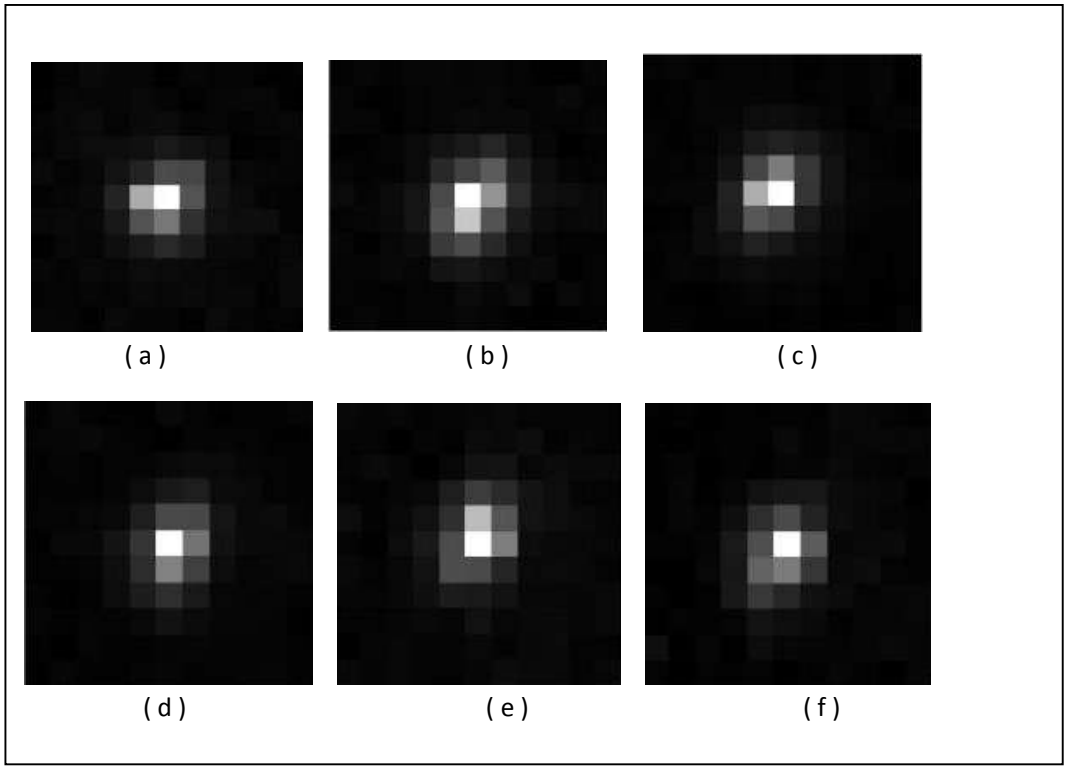

Figure 3 Star - Point Source observed by C2E PAN Sessions: 0, 1, 2, 3, 4, 5 (butting zone)

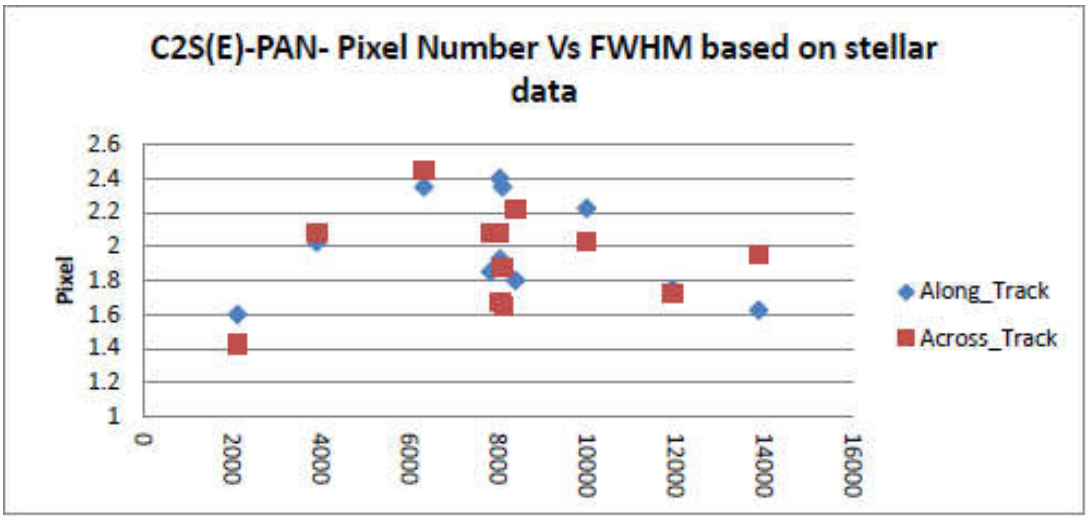

Plot1: Observed FWHM at different locations of the PAN detector array

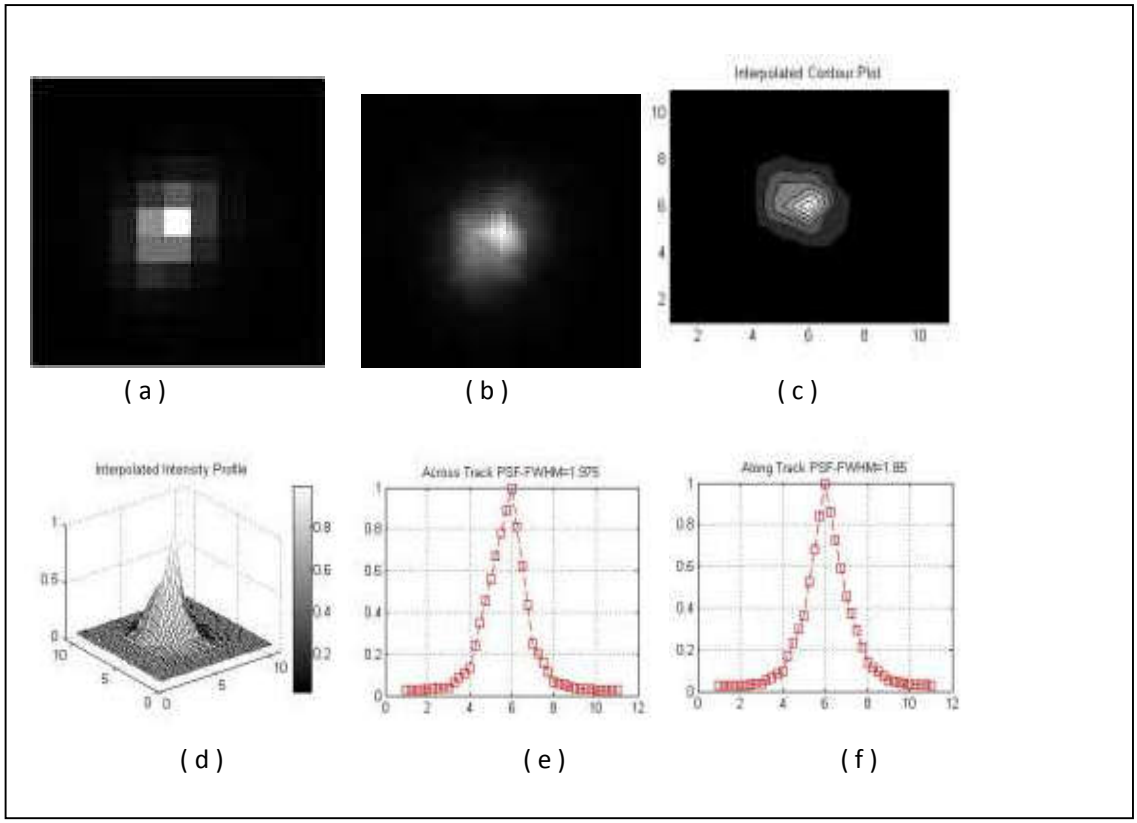

Figure 4 PAN Full Array (a) Integrated PSF, (b) Interpolated PSF, (c) Contour plot, (d) Intensity Profile, (e) Across track PSF plot, (f) Along track PSF plot

Similarly, for HRMX camera the observations made in two different dates in the normal detector array and butting zones using star 7840 for all the bands are used for characterising the individual bands of MX camera at the butting zones as it has four butting zones as well as non butting zone detector array. The FWHM variations across detector array for Band1 between 1.3 pixels to 2.5 Pixels. The star maximum intensity in DN counts is observed to be about 634 and varying upto a minimum of 264 DN counts at different segment of array as mentioned in Table4. The FWHM variations across detector array for Band2 between 1.4 pixels to 2.3 pixels. The star maximum intensity in DN counts is observed to be about 605 and varying upto a minimum of 311 DN counts at different segment of array as mentioned in Table4.

The FWHM variations across detector array for Band3 between 1.3 pixels to 2.1 Pixels. The star maximum intensity in DN counts is observed to be about 363 and varying upto a minimum of 200 DN counts at different segment of array as mentioned in Table5. The FWHM variations across detector array for Band 4 between 1.3 pixels to 1.9 Pixels. The star maximum intensity in DN counts is observed to be about 185 and varying upto a minimum of 120 DN counts at different segment of array as mentioned in Table5 for the non butting zones of array. Fig 5 and Fig 6 depict the spatial energy spread of point source in pixel positions for all the bands observed in session 4. All the session star profiles are not depicted due to the space constraint , however only qualified stars are considered for computing integrated PSF of individual bands as mentioned in the methodology. Plot2 shows the different FWHM observed for Band1 detector array. The integrated PSF is derived for Band1 in across track direction is 2 pixels and in along track direction is 1.8 pixels. Similarly for Band 2 integrated PSF is observed to be 2.0 pixels in across track direction and 1.9 pixels in along track direction, for Band3 in across track 1.7 pixels and 1.5 pixels in along track direction, for Band 4 in across track 1.5 pixels and 1.6 pixels in along track direction. Similarly, Plot3, plot4 and plot5 depict the intensity profiles observed at various locations of the array by Band2, Band3 and Band4.

Table 4 Estimated FWHM for Bands 1 and 2 of MX sensor in non-butting zone

Session No	Intended Location	Band-1			Band-2		
		DN Counts	Along track FWHM	Across track FWHM	DN Counts	Along track FWHM	Across track FWHM
0	2000	453	1.4	1.5	497	1.4	2
1	3200	634	1.4	1.3	605	1.4	1.8
2	4500	320	2.2	1.9	321	2.1	1.8
3	4800	335	1.6	2.1	311	2.1	2.3
4	6000	264	2.3	2.5	325	2.1	2.1

Table 5 Estimated FWHM for Bands 3 and 4 of MX sensor in non-butting zone

Session No	Intended Location	Band-3			Band-4		
		DN Counts	Along track FWHM	Across track FWHM	DN Counts	Along track FWHM	Across track FWHM
0	2000	259	1.375	1.5	138	1.975	1.425
1	3200	363	1.35	1.425	185	1.4	1.375
2	4500	220	1.55	1.85	120	1.575	1.5
3	4800	226	1.95	2	131	1.975	1.65
4	6000	200	1.65	2.175	144	1.75	1.625

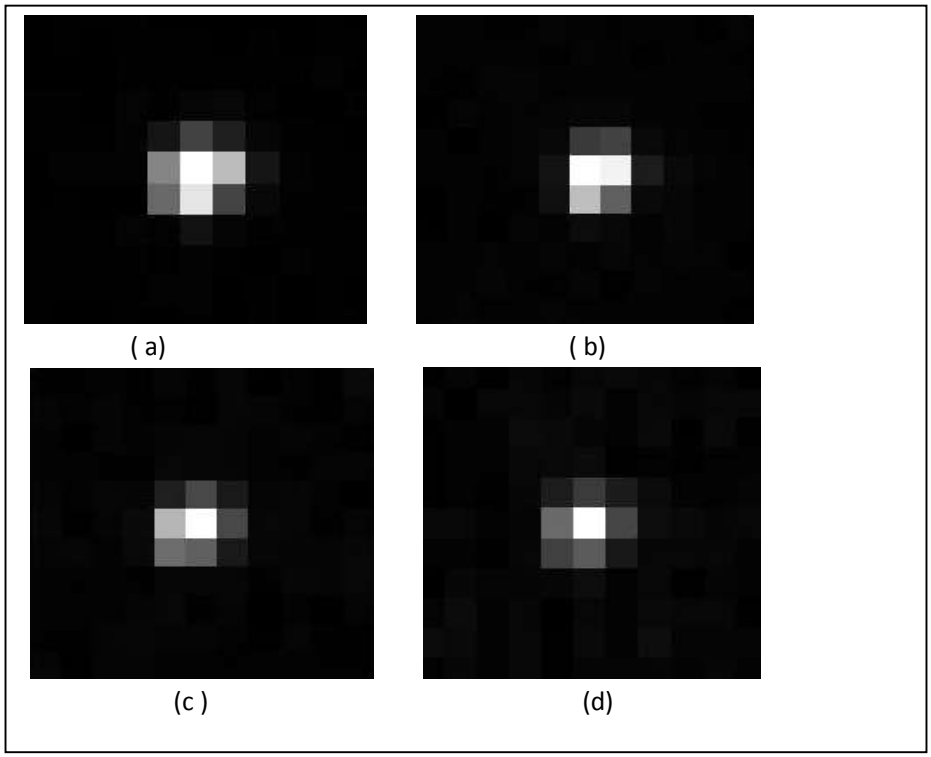

Figure 5 Star - Point Source observed by C2E MX Band -1,2,3,4 Sessions: 4 (non butting zone)

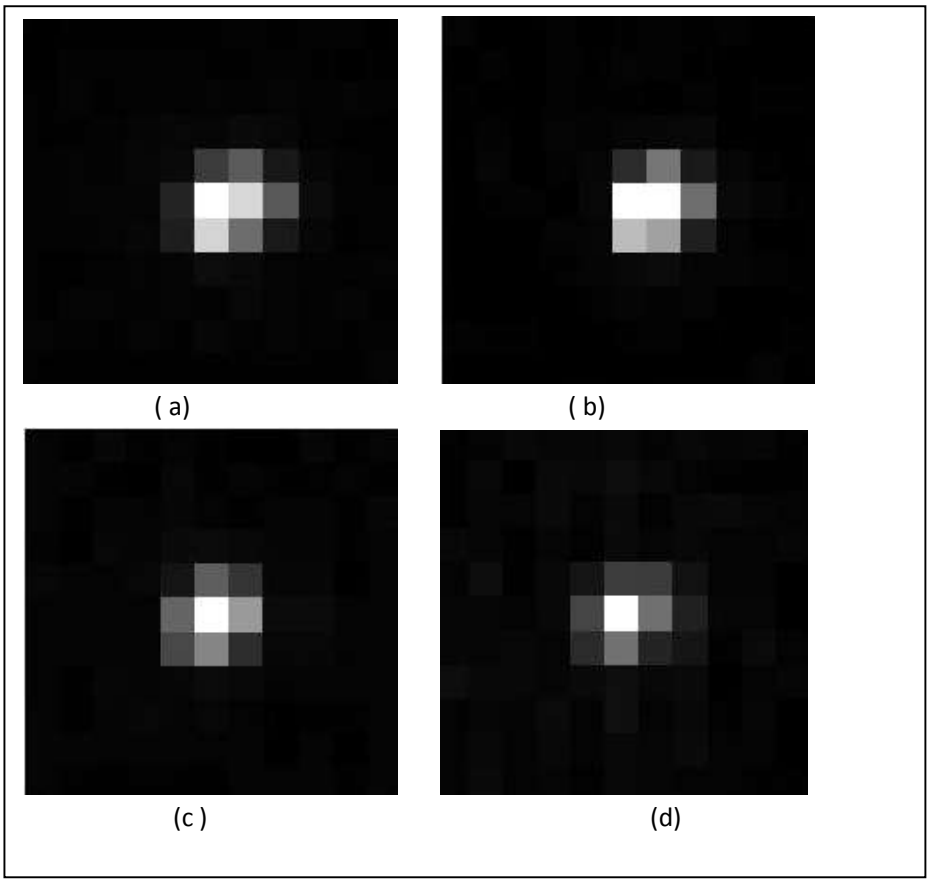

Figure 6 Star - Point Source observed by C2E MX Band -1,2,3,4 Sessions: 4 (butting zone)

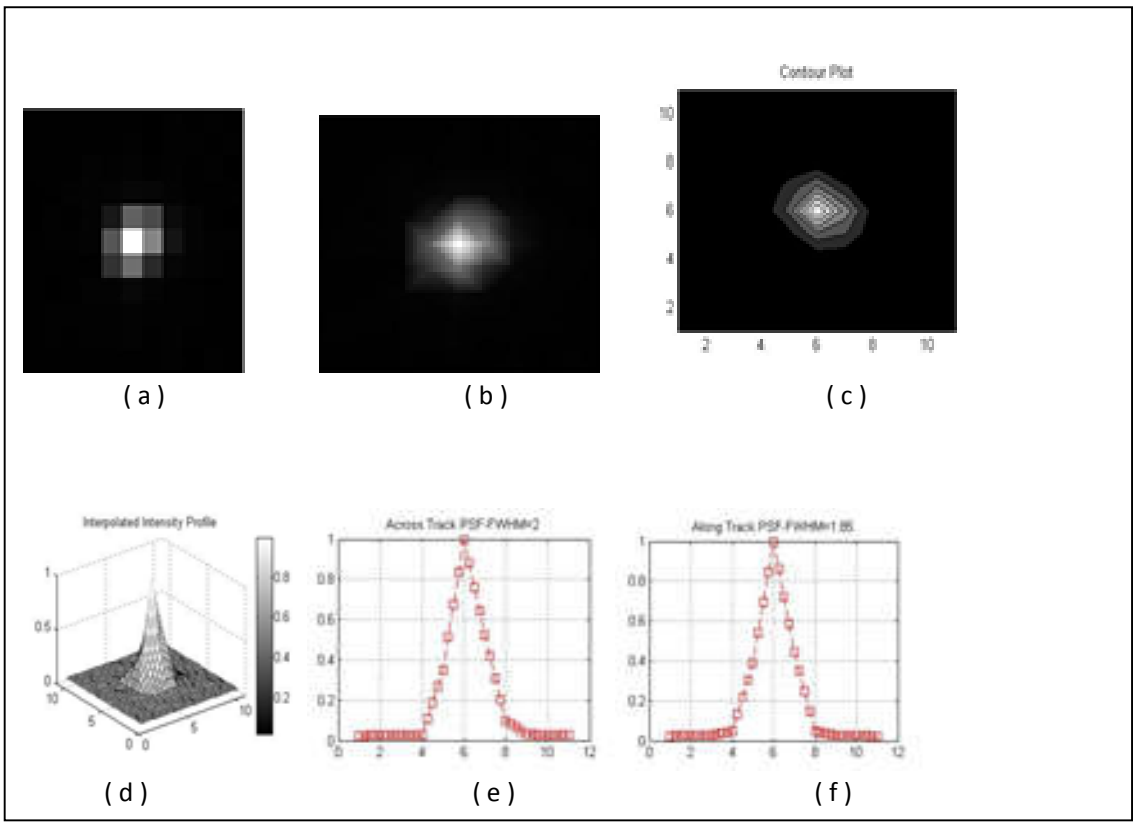

Figure 7 MX Band-1 Full Array (a) Integrated PSF, (b) Interpolated PSF, (c) Contour plot, (d) Intensity Profile, (e) Across track PSF plot, (f) Along track PSF plot

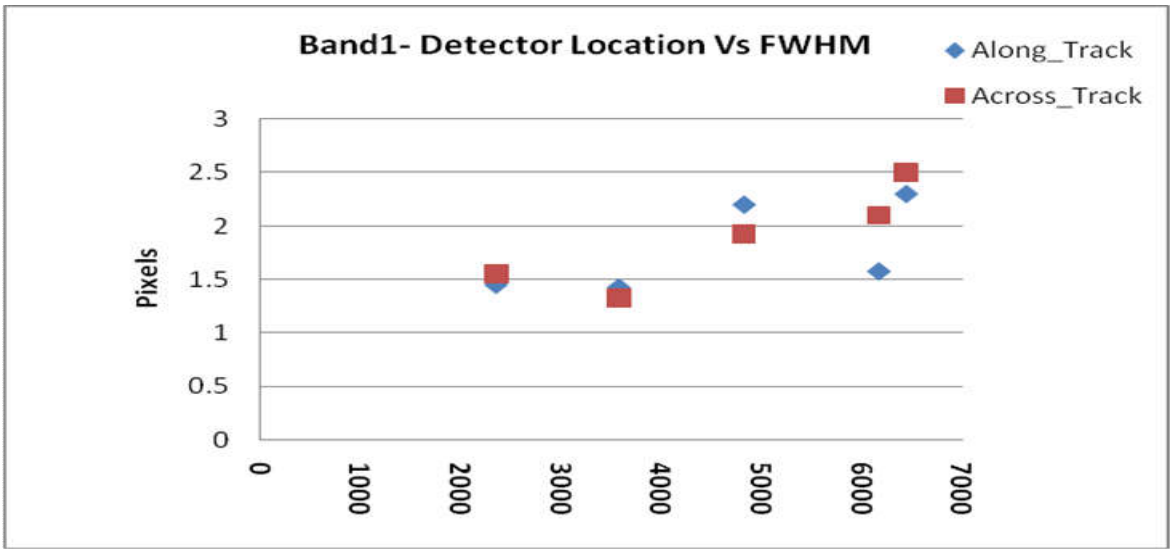

Plot2: Observed FWHM at different locations of the detector array of HRMX-Band1

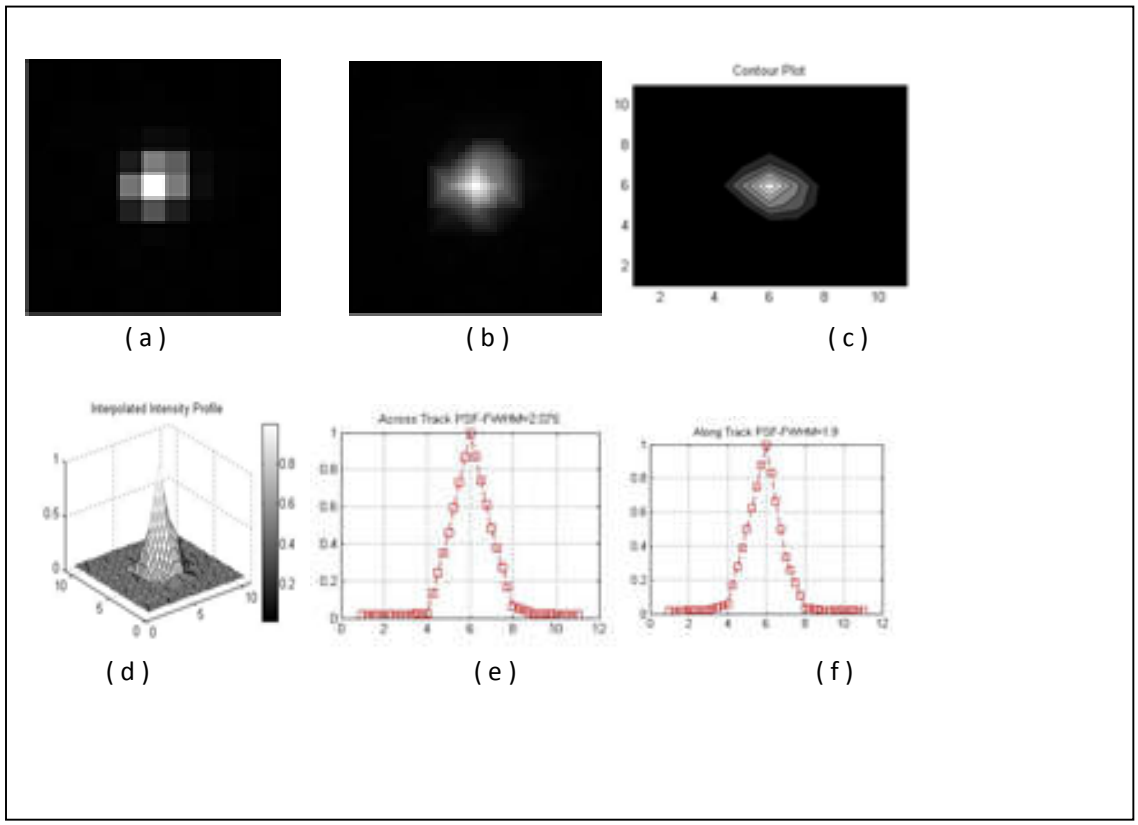

Figure 8 MX Band-2 Full Array (a) Integrated PSF, (b) Interpolated PSF, (c) Contour plot, (d) Intensity Profile, (e) Across track PSF plot, (f) Along track PSF plot

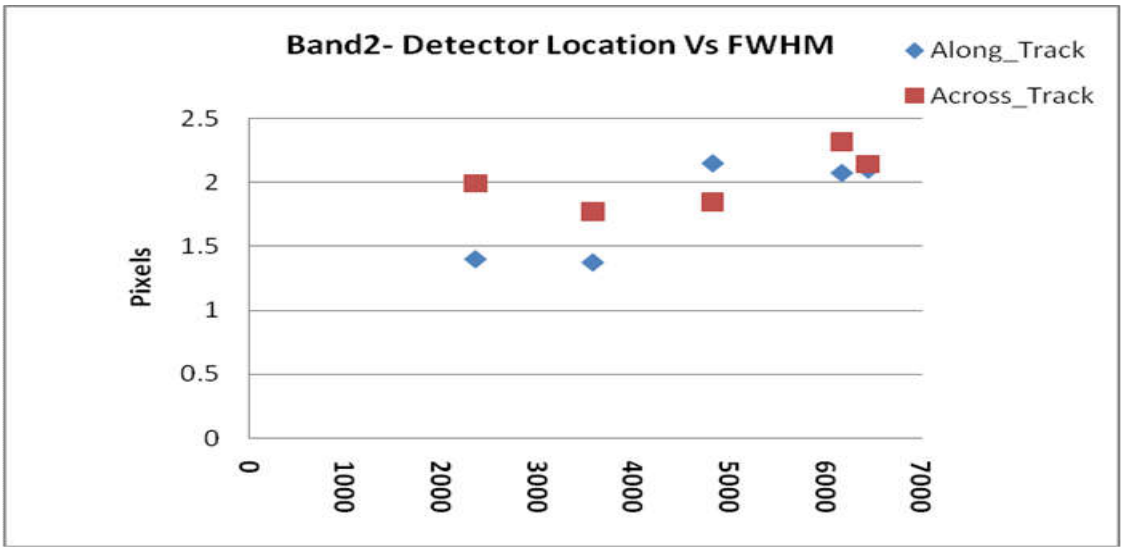

Plot3: Observed FWHM at different locations of the detector array of HRMX-Band2

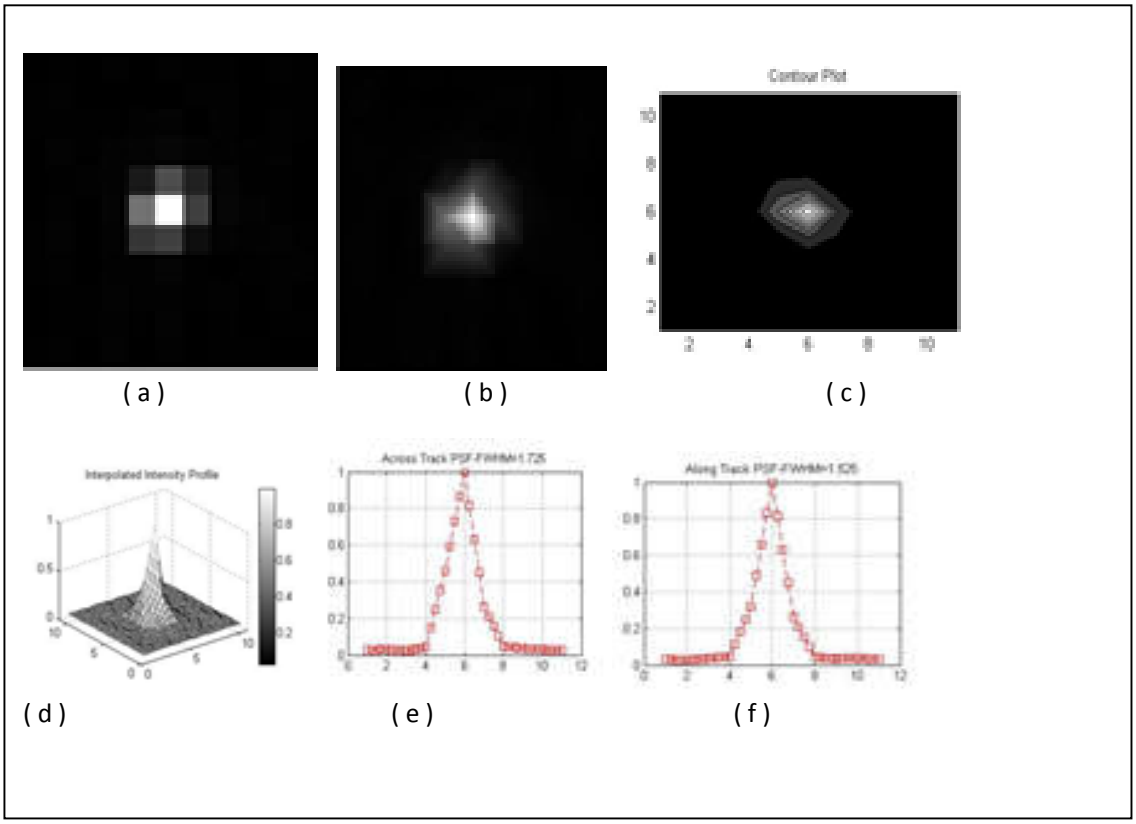

Figure 9 MX Band-3 Full Array (a) Integrated PSF, (b) Interpolated PSF, (c) Contour plot, (d) Intensity Profile, (e) Across track PSF plot, (f) Along track PSF plot

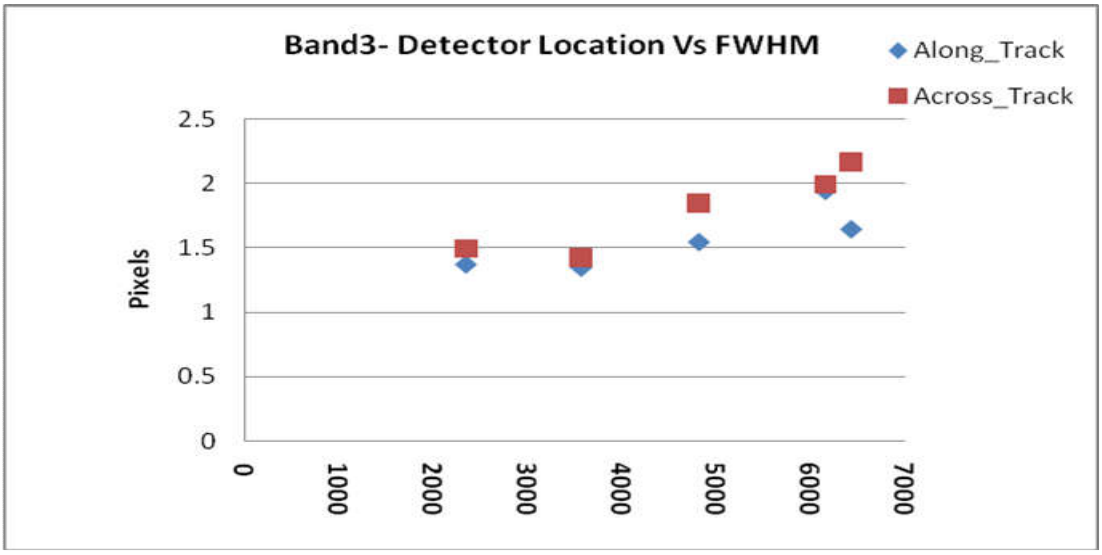

Plot4: Observed FWHM at different locations of the detector array of HRMX-Band3

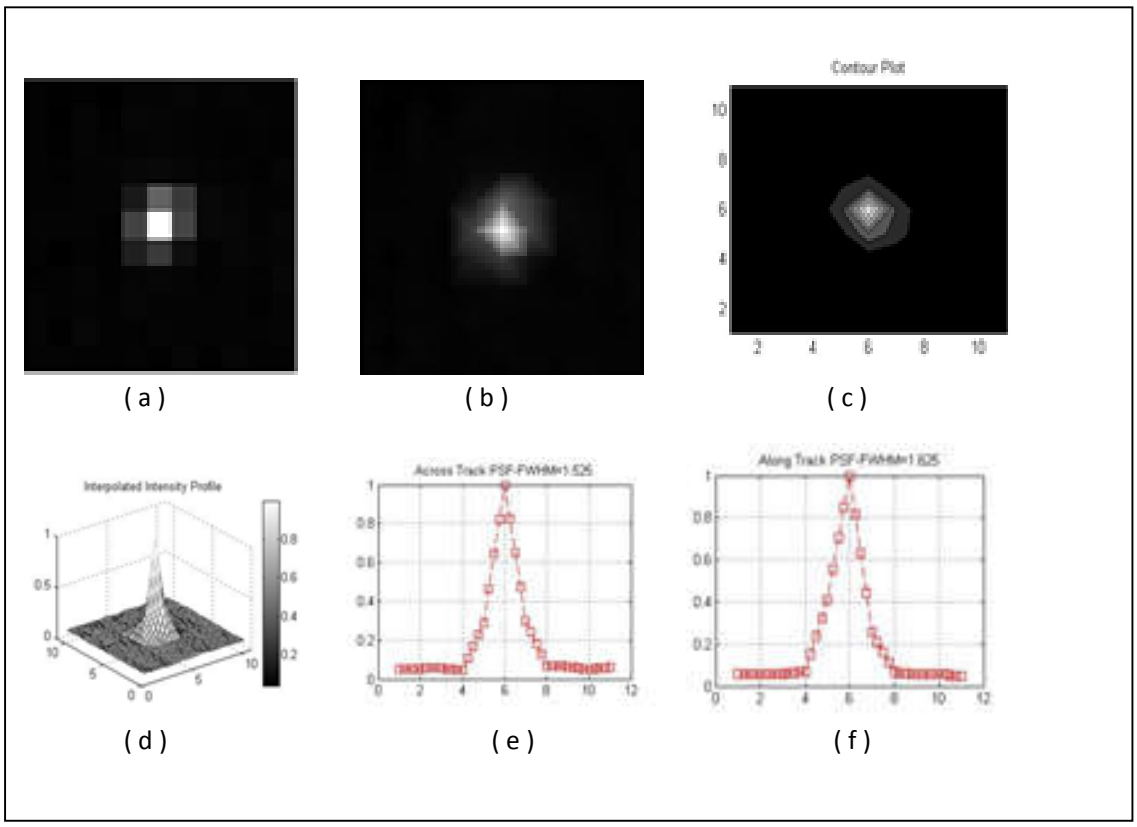

Figure 10 MX Band-4 Full Array (a) Integrated PSF, (b) Interpolated PSF, (c) Contour plot, (d) Intensity Profile, (e) Across track PSF plot, (f) Along track PSF plot

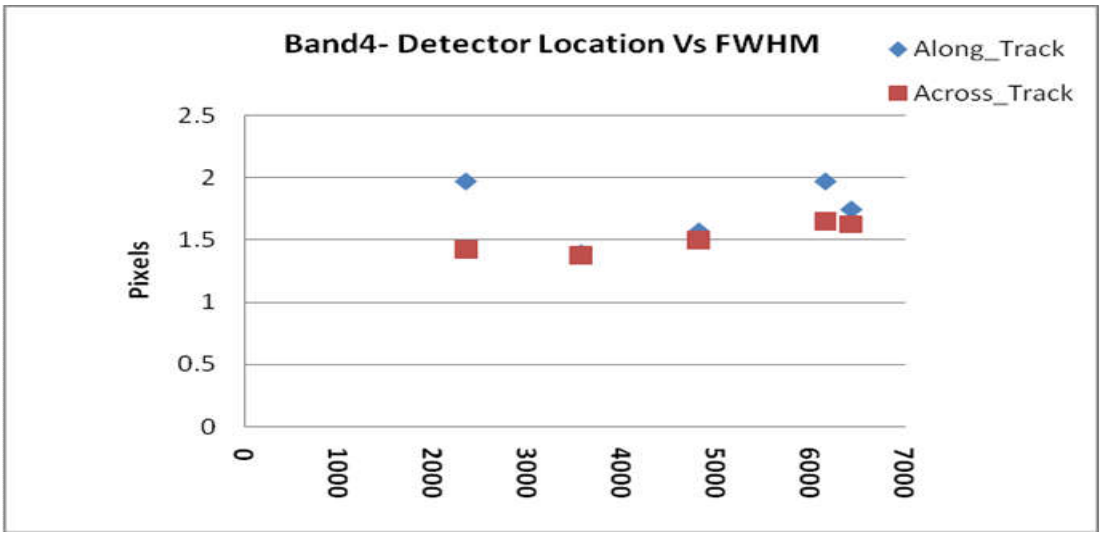

Plot5: Observed FWHM at different locations of the detector array of HRMX-Band4

7. CONCLUSIONS

- The integrated PSF computed for the array using qualified stars out of stellar observations is useful in establishing instrumental PSF in the orbit phase.
- The individual intensity profiles and respective FWHM derived using each star observation at different positions and sessions is useful in characterising the detector array fully and for observing any trends.
- The dark current can be arrived using deep space data where stars are not available. The system dark current is computed by integrating about 200 lines of deep space data where stars does not exists.
- The estimated instrumental PSF and system dark current in the early orbit phase can serve as a reference data and periodical estimation of these parameters(annually) will help in characterising degradations if any over a period throughout the operational phase.

ACKNOWLEDGEMENTS

Authors are grateful to Dr.Y.V.N.Krishna Murthy, Director, NRSC, for his guidance and encouragement during this work. We are thankful to C2S inter centre Project, Mission , Operations teams and for the timely support with data/services. Our special thanks are due to C2S, Project Director, Mission Director, Payload Team, SAC and Mission Team, ISAC for enabling and acquiring stellar mode data.

REFERENCES

1. https://calval.cr.usgs.gov/wordpress/wpcontent/uploads/Arnold_Robert_GE1_Stellar_Radiometric_Calibration_JACIE_April_2013_RevB.pdf
2. https://calval.cr.usgs.gov/wordpress/wp-content/uploads/26Bowen.pdf
3. Bowen, Howard, "Absolute Radiometric Calibration of the IKONOS Sensor Using Radiometrically Characterized Stellar Sources" ,Pecora 15/Land Satellite Information IV/ISPRS Commission I/FIEOS Conference Proceedings, 2002.
4. J. E. Gunn and L.L. Stryker, "Stellar Spectrophotometric Atlas", 3130<λ<10800A, Astrophysical Journal Supplement Series 52, 121-153, 1983.
5. H.S. Bowen and D.M. Cunningham, "Correction to Method of Establishing the Absolute Radiometric Accuracy of Remote Sensing Systems While On-orbit Using Characterized Stellar Sources" , JACIE2006.